ARTICLE NO. 79-4127

Airplane Brake-Energy Analysis and Stopping Performance Simulation

Mahinder K. Wahi*
Boeing Commercial Airplane Company, Seattle, Wash.

A digital simulation representing airplane dynamics under braking action has been developed. The basic equations of motion represent a rigid-body airplane with the forward, vertical, and pitch degrees of freedom. The landing-gear representation utilizes linear springs and dampers. Effects of engine transients, i.e., spinup and spindown, engine failure, reverse thrust, friction variation with velocity (wet runway), pitch dynamics and associated load transfer between gears, and flap-spoiler settings have been accounted for. The program is called LANRTO and is capable of computing maximum potential brake energies (100% braking efficiency) and stopping distances under landing and refused takeoff conditions for jet transport airplanes. The simulation is compatible with the certification procedures of both military (MIL-W-5013H and ASD-TR-68-56) and commercial (FAR 25, FAR 37/TSO-C26b) regulations. Good correlation has been achieved between results of this simulation and those of an analog-hardware brake control simulator.

Nomenclature

A_w = projected wing area, ft^2
BE_{tot} = brake energy 100%/wheel, ft-lb
BS_{ag} = body-station aft main gear
BS_{cg} = body-station c.g.
BS_{cgo} = body-station mean aerodynamic-chord leading edge
BS_{fg} = body-station forward main gear
BS_{ng} = body-station nose gear
C_d = aerodynamic-drag coefficient
C_l = aerodynamic-lift coefficient
C_n, C_1, C_2 = tire and strut-assembly damping coefficient for nose, forward main and aft main gears, respectively, lb-s/in.
E_m = total engine moment, pitch mode, ft-lb
F = net deceleration force, lb
F_{ag} = vertical load on the aft main gears, lb
F_d = aerodynamic drag force, lb
F_e = total engine thrust, lb
F_{ef} = thrust of the failed engine, lb
F_{eg} = forward thrust, lb
F_{er} = reverse thrust, lb
F_{fg} = vertical load on the forward main gears, lb
F_l = aerodynamic lift force, lb
F_m = main-gear retarding force, lb
F_n = nose-gear retarding force, lb
F_{ng} = vertical load on the nose gear, lb
g = acceleration due to gravity, in./s^2
h_l = height above ground of c.g., in.
I_{yy} = airplane pitch moment of inertia, in.-lb-s^2
k_n, k_1, k_2 = tire and strut-assembly vertical spring rates for nose, forward main and aft main gears, respectively, lb/in.
l_n, l_1, l_2 = distance between c.g., and nose, forward main and aft main gears, respectively, in.
M = airplane mass, slugs
mac = mean aerodynamic chord, in.
NB_{mg} = number of braked wheels, main gears
NW_{mg} = number of wheels, main gears
P_{mac} = c.g. as percent mac
S_{rc} = speed at thrust-reverser cutoff, knots
T_{bo} = time to brakes on, s
T_{ec} = time to engine cut, s
v_W = head or tail wind component, head wind positive, knots
v_l = touchdown or engine-failure velocity, knots
v_2 = airspeed ($v_l + v_W$), knots
W = airplane weight, lb
x = braking distance, positive forward, ft
y = airplane vertical displacement, positive downward, ft
Z_i = height below c.g., inboard or center engine, in.
Z_0 = height below c.g., outboard or pod engine, in.
θ = airplane pitch angle, positive clockwise, deg
σ = ρ/ρ_0, air-density ratio
ρ = ambient air density, lb-s^2/in.^{4}
ρ_0 = air density at sea level, std day, lb-s^2/in.^{4}
μ_{av} = available or torque-limited friction
μ_{app} = apparent or equivalent friction
$\mu_{max.}$ = maximum value of friction
$\mu_{min.}$ = minimum value of friction
μ_m = friction developed at main-gear tires
μ_n = friction developed at nose-gear tires
μ_r = rolling friction
$(\dot{\ })$ = differentiation with respect to time

Received Sept. 14, 1978; revision received Feb. 9, 1979.

Index categories: Simulation, Deceleration Systems, Landing Dynamics.

*Senior Engineer, Landing Gear Systems.

Introduction

THE aircraft manufacturer is faced with designing an optimum (minimum weight) braking system on one hand and meeting various certification requirements[1-3] on the other. A brake-energy analysis is utilized for sizing the brakes during the development of an airplane and later to predict and verify its stopping performance.

Previous estimates of airplane brake energy required tedious hand calculations either by iteration or exact solution of linearized equations. Since the problem is highly nonlinear, approximate solution required segmentation of the braked roll with separate calculations for each segment. Over the past several years many of the problems associated with this analysis have been computerized for obvious reasons. The present paper is one such attempt where a unified approach is taken to account for most, if not all, important parameters affecting brake-energy analysis.

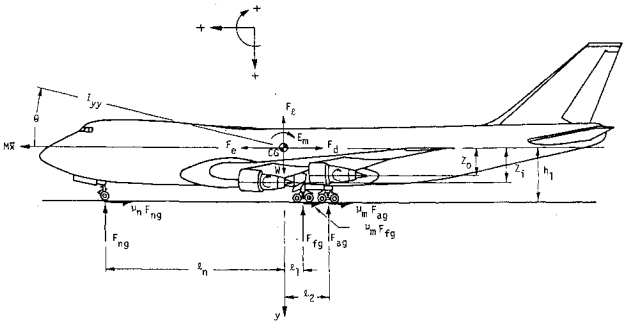

Fig. 1 Airplane dynamics model.

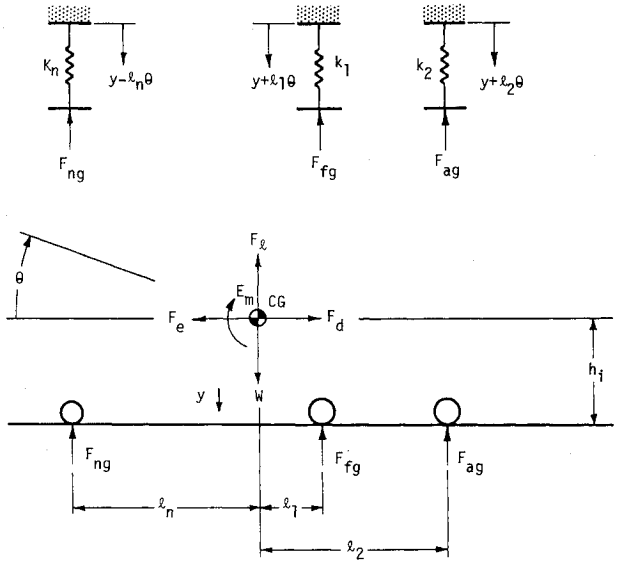

Fig. 2 Static equilibrium free-body diagram.

The analysis is compatible with Method II analysis requirements of Refs. 1, 2, and 3 and also meets many of the criteria specified in Refs. 4 and 5. A digital computer program called LANRTO was developed based on the analysis presented here and its validity is later shown by correlation. The program was coded in FORTRAN IV for the CDC 6600 computer.

For a given gross weight, temperature, and altitude, the program solves second-order differential equations of motion by summation of the aerodynamic and external braking forces acting on the airplane. Solution is accomplished using a Runge-Kutta variable step-size method, with time as the independent variable for a range of ground-friction coefficients. Input information on engine-thrust characteristics, airplane dimensions, spoiler and reverser actuation delay times, initial (touchdown or engine failure) velocities, and aerodynamic parameters is required. Where applicable, these inputs are in the form of tables. User option for the inclusion of nose-gear brakes is available. The equations as used in the program are derived here. For reasons explained in the discussion, the simulation does not account for the effects of skid-control system, i.e., a 100% braking efficiency is assumed and landing-gear strut and tires are treated as linear springs and dampers.

Analysis

Although assisted by aerodynamic drag and engine reverse thrust, slowing and stopping a modern aircraft on the ground is achieved principally by the use of wheel brakes to generate a horizontal drag force between the tires and the ground. In the braking process, the aircraft kinetic energy is converted to heat energy in the brakes by the application of hydraulic

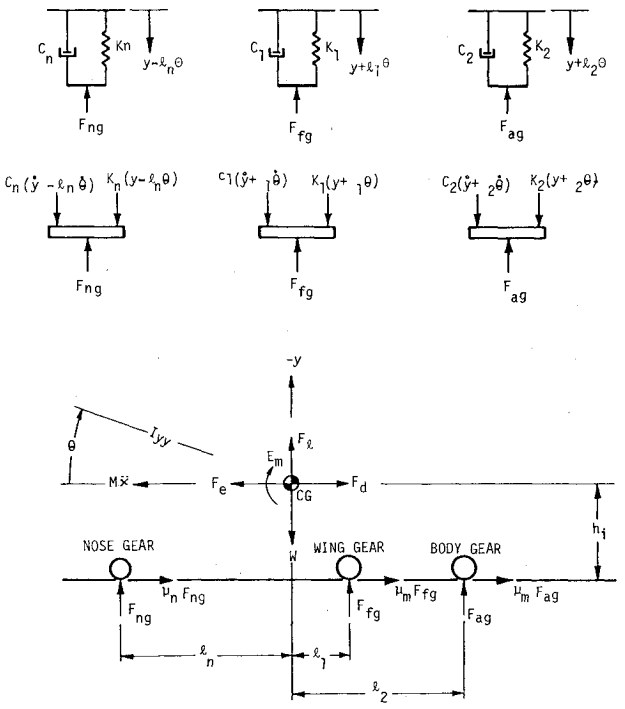

Fig. 3 Dynamic equilibrium free-body diagram.

power to the brake disks to create friction. The heat energy is dissipated by natural or forced cooling.

To evaluate properly the effective retarding forces on an airplane with thrust reversers available, it is necessary to isolate the component retarding forces. The component retarding forces consist of: 1) rolling resistance; 2) aerodynamic drag; 3) ram drag; 4) engine reverser thrust (if used); and 5) braking force. The other forces acting on the airplane are lift, weight, and forward idle thrust. A pictoral representation of the various forces is shown in Fig. 1. The analysis assumes a rigid airplane with 3 deg of freedom, namely vertical, y, horizontal, x, and rotation, θ. The vertical and rotational degrees of freedom are coupled and comprise the airplane pitching dynamics. Instead of treating both forward (e.g., wing) and aft (body) main gears lumped together, (the usual practice) they are treated as independent main gears (see Fig. 1).

The vertical ground-reaction force is assumed to be equal for all main-gear wheels on a given gear and is computed by taking moments of all considered forces acting on the airplane, including the aerodynamic lift and drag. The brake-retarding force per wheel is then the vertical reaction force multiplied by the available ground-friction coefficient between the tire and the runway surface. For the case of an unbraked wheel, the free rolling-friction coefficient is used. Similar calculations are performed for the nose-gear wheels, which are assumed to act as a point.

The total retarding force at the wheels is summed with the engine thrust and the aerodynamic drag to produce the resultant instantaneous force acting on the airplane mass. Solution of the differential equations of motion with respect to time provides a time history of the airplane parameters from an initial velocity to stop. The total energy per brake is then the integral over the time interval of the instantaneous brake drag force for the wheel times the instantaneous airplane velocity.

Airplane Pitching

Airplanes for which the ratio of center-of-gravity height, h_1, to wheelbase, $[l_n + (l_1 + l_2)/2]$, is high, have a large weight transfer to the nose wheel while braking. This weight transfer limits the braking ability of the airplane since it

reduces the vertical reaction between the main-gear tires and the ground. To account for this pitching-mode operation, a three degree-of-freedom model, Fig. 1, of the airplane is used.

In the analysis that follows, the tire-strut assembly is considered as a spring-damper system, with equivalent spring rates, k_n, k_1, k_2, and equivalent damping coefficients, C_n, C_1, C_2, respectively, for the nose, forward main, and aft main gears (see Figs. 2 and 3).

Figure 1 shows the geometric arrangement of all the forces and moments considered to act on the airplane. Horizontal distances are measured from a vertical plane through c.g. and vertical distances are measured from the ground or from a horizontal plane through c.g. All forces are assumed to be either parallel or perpendicular to the ground lines. The ground-reaction forces are assumed to act through the centerlines of the nose and each set of main gears; the aerodynamic-lift and drag forces and the airplane weight act through the center of gravity; the engine thrust acts through a line at the mean engine height; and the braking forces between the tires and the ground act at the centerlines of the nose and main gears.

Static Equilibrium

Considering the airplane at rest, Fig. 2 shows the free-body diagram for static equilibrium. Summing forces in the vertical direction gives

$$F_{\text{vert}} = 0 = (W - F_l) - (F_{ng} + F_{fg} + F_{ag}) \tag{1}$$

and summing moments about the center of gravity gives

$$M_{cg} = 0 = F_{ng} l_n - F_{fg} l_1 - F_{ag} l_2 + E_m \tag{2}$$

The three vertical gear loads may be written as (see Fig. 2)

$$F_{ng} = k_n (y - l_n \theta)$$

$$F_{fg} = k_1 (y + l_1 \theta)$$

$$F_{ag} = k_2 (y + l_2 \theta)$$

Substituting for F_{ng}, F_{fg}, and F_{ag} into Eqs. (1) and (2) and rearranging terms, we get:

$$(k_n + k_1 + k_2) y - (k_n l_n - k_1 l_1 - k_2 l_2) \theta = (W - F_l) \tag{3}$$

$$-(k_n l_n - k_1 l_1 - k_2 l_2) y + (k_n l_n^2 + k_1 l_1^2 + k_2 l_2^2) \theta = E_m \tag{4}$$

Solving Eqs. (3) and (4) simultaneously and rearranging denominator terms, we get:

$$y = [(W - F_l)(k_n l_n^2 + k_1 l_1^2 + k_2 l_2^2) + E_m (k_n l_n - k_1 l_1 - k_2 l_2)]$$
$$/ [k_n k_1 (l_n + l_1)^2 + k_n k_2 (l_n + l_2)^2 + k_1 k_2 (l_1 - l_2)^2)] \tag{5}$$

$$\theta = [(W - F_l)(k_n l_n - k_1 l_1 - k_2 l_2) + E_m (k_n + k_1 + k_2)]$$
$$/ (k_n k_1 (l_n + l_1)^2 + k_n k_2 (l_n + l_2)^2 + k_1 k_2 (l_1 - l_2)^2] \tag{6}$$

Equations (5) and (6) give the static values of airplane vertical and rotational displacements at time zero and thus are the initial conditions for the dynamic differential equations.

Dynamic Equilibrium

Under dynamic conditions, the free-body diagram could be shown as in Fig. 3. The total instantaneous accelerating force acting through the center of gravity is the sum of all the horizontal forces, i.e.,

$$\sum F_{\text{hor}} = M\ddot{x} = F_e - F_d - \mu_n F_{ng} - \mu_m (F_{fg} + F_{ag}) \tag{7}$$

Summation of all the vertical forces gives

$$\sum F_{\text{vert}} = M\ddot{y} = W - F_l - F_{ng} - F_{fg} - F_{ag} \tag{8}$$

and summation of moments about the center of gravity gives

$$\sum M_{cg} = I_{yy}\ddot{\theta} = \{F_{ng} l_n - F_{fg} l_1 - F_{ag} l_2$$
$$- h_l [F_{ng} \mu_n + (F_{fg} + F_{ag}) \mu_m] + E_m\}$$

or

$$I_{yy}\ddot{\theta} = [(l_n - \mu_n h_1) F_{ng} - (l_1 + \mu_m h_1) F_{fg}$$
$$- (l_2 + \mu_m h_1) F_{ag} + E_m] \tag{9}$$

The three vertical gear loads may be written as (see Fig. 3)

$$F_{ng} = k_n (y - l_n \theta) + C_n (\dot{y} - l_n \dot{\theta}) \tag{10}$$

$$F_{fg} = k_1 (y + l_1 \theta) + C_1 (\dot{y} + l_1 \dot{\theta}) \tag{11}$$

$$F_{ag} = k_2 (y + l_2 \theta) + C_2 (\dot{y} + l_2 \dot{\theta}) \tag{12}$$

Rewriting Eqs. (7), (8), and (9) in terms of F_{ng}, F_{fg}, and F_{ag}, we get:

$$\ddot{x} = [F_e - F_d - \mu_n F_{ng} - \mu_m (F_{fg} + F_{ag})] / M \tag{13}$$

$$\ddot{y} = (W - F_l - F_{ng} - F_{fg} - F_{ag}) / M \tag{14}$$

$$\ddot{\theta} = [(l_n - \mu_n h_1) F_{ng} - (l_1 + \mu_m h_1) F_{fg}$$
$$- (l_2 + \mu_m h_1) F_{ag} + E_m] / I_{yy} \tag{15}$$

Equations (10) through (15) may be solved to determine the instantaneous dynamic values of x, y, θ, and other parameters.

Engine Thrust F_e

In the refused takeoff (RTO) condition it is assumed that if one engine fails at the v_1 speed, the other engines are cut simultaneously after a delay time of T_{ec} seconds. Thus, the engines decay with time as a percentage of their initial thrust until idle thrust is reached. Initial thrust and idle thrust are functions of installed takeoff thrust and are dependent on ambient conditions of temperature and altitude and on airplane velocity.

Thus for a four-engine airplane, the total engine thrust may be determined as a function of time T as:

$$F_e = 3F_{et} + F_{ef} \quad \text{for} \quad T < T_{ec}$$

and

$$F_e = 3F_{eg} + F_{ef} \quad \text{for} \quad T \geq T_{ec}$$

In the landing condition, the takeoff thrust is replaced by flight idle thrust where flight idle values are higher than the ground idle values. At touchdown (time = zero) the engines will possess flight idle values and then spin down to ground idle using the percentage decay factor.

Reverse Thrust

The amount of thrust applied at any point during the landing roll is given by the schedule of operation. The schedule (see Fig. 4) includes the time delay after touchdown for reverser actuation, reverse engine acceleration, time at maximum reverse thrust, and engine deceleration from a prescribed cutoff ground speed. The percent applied thrust is

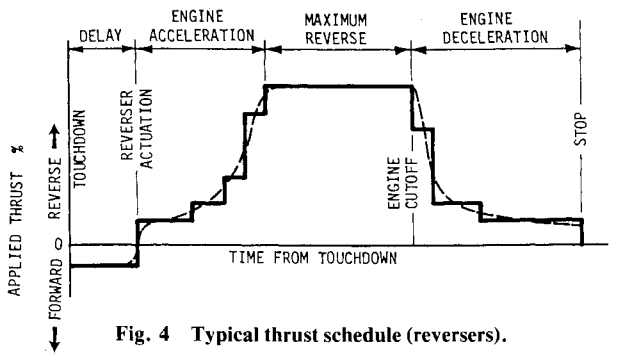

Fig. 4 Typical thrust schedule (reversers).

the percentage of a given thrust curve which varies with velocity. This is actually a continuous function, as shown in Fig. 4 by the dashed line for a typical thrust schedule, but may be approximated by a time-step function (the usual approach). In the current analysis, however, these engine transients were accounted for by a first-order lag for engine deceleration (thrust decay or spindown) and a second-order lag for engine acceleration (thrust buildup or spinup) and these representations are based on actual engine test data. Typical landing and RTO cases using this engine model are shown in Figs. 5 and 6.

The (fan and primary) thrust reversers produce in reverse about 40 to 50% of the engine forward thrust when operated at the maximum engine rating. Because the thrust reversers produce a flowfield with a forward velocity which reduces airplane drag and engine ram drag, the full effect of the 40 to 50% is not realized by the airplane. This interference loss represents approximately 20 to 40% of the attainable reverse thrust and varies with speed. With this understanding, the equation for reverse thrust may be written as follows:

$$F_{er} = (F_{rg}E_1 + R_d)E_2 \tag{16}$$

where

F_{rg} = gross reverse thrust

E_1 = reverser effectivity (e.g., $\cdot 4$ to $\cdot 5$)

R_d = ramdrag

E_2 = interference loss correction factor (e.g., $\cdot 6$ to $\cdot 8$)

The values for E_1 and E_2 included here are arbitrary and vary from airplane to airplane. Actual test data must be used whenever available.

Engine Pitching Moments

Since the airplane dynamics model includes airplane pitching mode it is only appropriate that the contribution made by the engine pitching moments be included [see Eqs. (2) and (9)]. For the landing condition with no failed engines and with or without reverse-thrust usage, the net engine moments would be

$$E_m = F_e(Z_i + Z_0)/2 \quad \text{for two- and four-engine airplanes} \tag{17}$$

and

$$E_m = F_e(2Z_0 + Z_i)/3 \quad \text{for three-engine airplanes} \tag{18}$$

It should be noted that $Z_i = Z_0$ for two-engine airplanes and Z_i is the moment arm of the center engine for a three-engine airplane. It is also assumed that only symmetrical reverse thrust is applied.

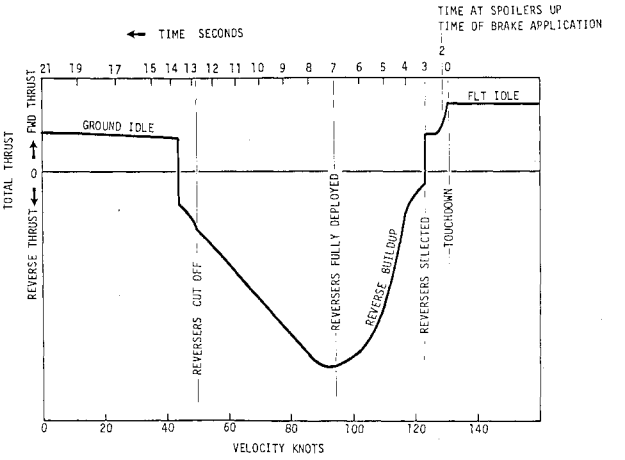

Fig. 5 Typical landing with four engines in reverse.

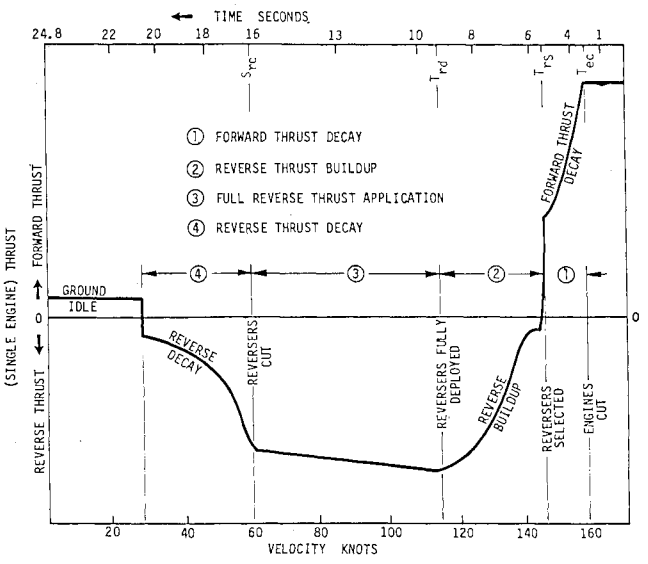

Fig. 6 Typical RTO with two engines in reverse.

In an RTO condition, asymmetrical thrust/moments are generated at engine failure (except with center engine failed in a three-engine airplane) and quite a few options are available to the pilot, depending upon location of engine failure (outboard or inboard), number of engines on the airplane (two, three, or four), and reverse-thrust usage (one, two, or three engines or none). To keep analysis handling reasonably simple it was assumed that the pilot would apply only symmetrical reverse thrust or none at all, just as for landing configuration. For brevity, the logic and equations are not included here.

Center-of-Gravity Calculations

The airplane center of gravity is calculated as a function of percent mean aerodynamic chord (% mac) with various body-station inputs needed for the individual gears and the mac leading edge (see Fig. 7). The equations used are as follows:

$$BS_{cg} = BS_{cg0} + \text{mac}(P_{\text{mac}})$$

where P_{mac} = percent mean aerodynamic chord fraction (e.g., 12% = $\cdot 12$)

$$l_1 = BS_{fg} - BS_{cg}$$

$$l_2 = BS_{ag} - BS_{cg}$$

$$l_n = BS_{cg} - BS_{ng}$$

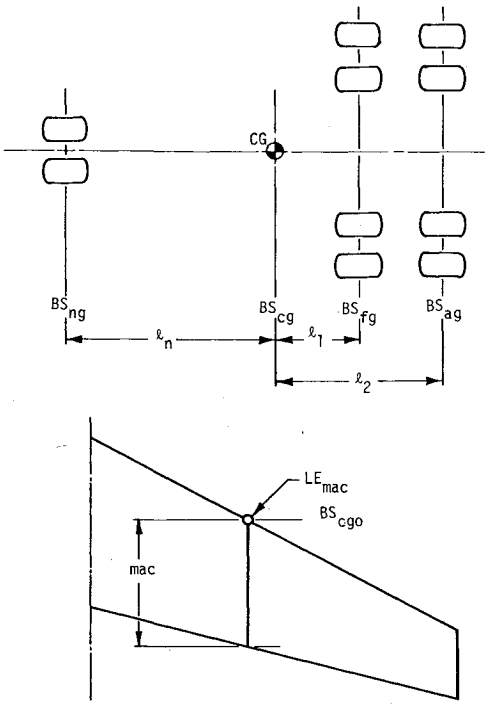

Fig. 7 Definition of c.g. terms.

Aerodynamic Drag Force F_d and Lift F_l

The lift and drag forces are calculated as functions of the lift and drag factors K_l and K_d, the air-density ratio σ, and the airstream velocity v_2 (true airspeed) as follows:

$$v_2 = v_l + v_W \qquad \sigma = \rho/\rho_0$$

$$K_l = \rho_0 C_l A_W/288 \qquad K_d = \rho_0 C_d A_W/288$$

$$F_l = \sigma K_l v_2^2 \qquad F_d = \sigma K_d v_2^2$$

Developed Ground-Friction Coefficient

For each set of input conditions, brake energy and stopping distance are calculated for a specific range of developed ground-friction coefficients. Thus the friction coefficient is varied from a minimum value of $\mu_{\min.}$ through increments $\mu_{\text{inc.}}$ to a maximum value of $\mu_{\max.}$. The free-rolling coefficient is defined as μ_r and the general value of friction coefficient as μ.

For the main gear, the average developed friction coefficient after brake application is defined as:

$$\mu_{mm} = \mu NB_{mg}/NW_{mg} + \mu_r(1 - NB_{mg}/NW_{mg})$$

where

NW_{mg} = number of wheels on main gear

NB_{mg} = number of braked wheels on main gear

μ = developed ground-friction coefficient

Then for the normal case of all main-gear wheels being braked:

$$\mu_{mm} = \mu$$

and for 50% brake failure:

$$\mu_{mm} = \mu/2 + \mu_r/2$$

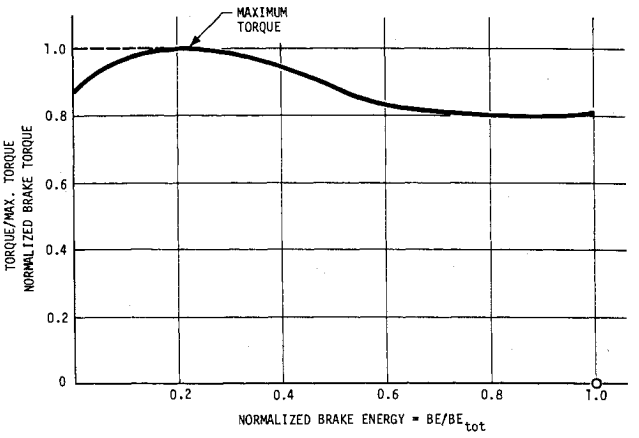

Fig. 8 Typical brake energy vs torque curve.

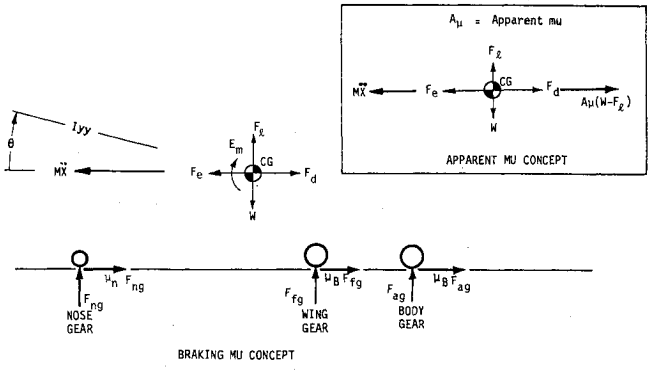

Fig. 9 Apparent and braking μ concepts.

For the nose gear

$\mu_{mm} = \mu_r$ for the case with no nose-wheel brakes

and

$\mu_{mm} = \mu$ for the case with nose-wheel brakes

Assuming a time delay of T_{b0} seconds from v_1 speed to brakes on, the developed ground-friction coefficient for each wheel on the main gear is then:

$$\mu_m = \mu_r \quad \text{for} \quad T < T_{b0}$$

$$\mu_m = \mu_{mm} \quad \text{for} \quad T \geq T_{b0}$$

Brake-Retarding Force and Brake Energy

As previously defined in Eq. (7), the brake-retarding force is

$F_n = \mu_n F_{ng}$ for the nose-gear wheels

$F_m = \mu_m(F_{fg} + F_{ag})$ for the main-gear wheels

The rate of change of brake energy is then:

$$\dot{W}_b = F_m \dot{x} \text{ for the main gear wheels}$$

where $\dot{x}$ is the instantaneous airplane velocity.

Integrating this equation over the braked roll yields the brake energy absorbed per wheel.

The known parameters BE_{tot} (total brake energy/wheel, see Fig. 8), $TOR_{\max.}$ (maximum available torque/wheel), and NW_{mg} are used to determine whether the braking phenomenon is torque-limited or friction-limited. The in-

Table 1 Comparison of braking segment distances in feet[a]

Model	Medium-range jet		Short-range jet		Long-range jet		Military transport		Fighters	
μ	Ref. (6)	LANRTO	Ref. (6)	LANRTO	Ref. (6)	LANRTO	Ref. (6)	LANRTO	Ref. (6)	LANRTO
0.6	1087	1079	914	931	1709	1707	1227	1227	1876	1878
0.5	1259	1257	1063	1085	1983	1983	1418	1407	2103	2104
0.4	1505	1500	1280	1296	2382	2378	1693	1692	2415	2420
0.3	1893	1885	1626	1642	3015	3018	2123	2112	2878	2864
0.2	2595	2583	2263	2244	4183	4175	2897	2878	3645	3649
0.1	4321	4317	3883	3869	7189	7173	...	...	...	...
Wet (0.05 to 0.5)	3328	3324	...	...	5961	5943	...	...	...	...

[a] The distances shown are for perfect stops, i.e., 100% efficient antiskid system.

stantaneous computed brake energy is normalized to obtain percent torque (Fig. 8). The percent torque is multiplied by $TOR_{max.}$ to obtain actual torque per wheel, and this is converted to torque force using tire-torque radius. The actual torque force is then compared with the brake-retarding force F_m, and if torque-limited, the value of available μ is adjusted downward.

Apparent μ

A user option allows the program to be run for a braking μ or apparent μ configuration; the two concepts are shown in Fig. 9. The apparent μ configuration concept is useful in preliminary design work, where the gear footprint and individual gear locations may not be known. A similar concept is also used in computing an equivalent μ value from given flight-test data where stopping distance and other relevant information is known, the results being used to define airplane performance. The apparent μ concept is based on gear geometry (static load transfer) alone, and the equation used to calculate it is as follows:

$$\mu_{app} = \mu_{av} l_n / [l_n + 0.5(l_1 + l_2) + \mu_{av} h_1] \qquad (19)$$

where μ_{av} = available μ or torque-limited μ.

This definition of apparent μ is compatible with that of Ref. 5.

Wet Runway

A variable μ option is included (e.g., for wet runways) where a user-defined μ-velocity table input defines runway friction.

Program Verification

The program has been verified by case runs with all available options. More specifically, case runs were made with no failed engines, outboard failed engine, inboard failed engine; no reverse thrust, symmetrical reverse thrust; apparent μ, braking μ; dry runway, wet runway; two-engine airplane, three-engine airplane, and four-engine airplane configurations. In addition, braking distances obtained from an analog-hardware brake-control simulator (Ref. 6), for five airplanes were compared with those obtained by the program LANRTO, and the comparison is shown in Table 1 (also see Discussion). The difference in results is less than 1% in all cases. The correlation is thought to be very satisfactory.

Braking μ-Apparent μ Correlation

When a case run is made with braking μ option, the program calculates an equivalent apparent μ value using Eq. (19); conversely, the program calculates an equivalent braking μ for a run made with an apparent μ option.

The accuracy of Eq. (19) was verified as follows: 1) make a run with a braking μ value, e.g., $\mu = 0.4$. This gives an equivalent $\mu_{app} = 0.333$; $S = 2848$ ft, and 2) make same run with apparent μ option with $\mu = 0.333$. This gave $S = 2853$ ft.

Discussion

Assumptions

Two major assumptions were made for the present analysis: 1) effects of the skid-control system (efficiency) on stopping performance were not considered; and 2) linear spring-and-damper representation was used for the gear struts and tires. The reasons for these asumptions are discussed below.

The effects of a skid-control system on an airplane's stopping performance can vary greatly and are normally expressed in terms of braking-efficiency curves[7] obtained through real time dynamic simulations. Over the past several years the Boeing Co. has developed an analog-hardware brake-control simulator[6] and used it for brake-system evaluation, tuning, and development on virtually all jet transports. An integral part of its use has been through verification that system performance on the computer matches that obtained during airplane flight tests. The correlation consisted of comparing stopping distances, skid pressures, number, depth and rate of skids, strut fore and aft frequencies and airplane pitching frequencies and damping ratios.

Obviously, such complex dynamics of a skid-control system cannot be easily represented in a digital simulation. After establishing the correlation for known flight-test conditions, the stopping distance for a 100% efficient braking system such as those shown in Table 1 were established. These flight test-simulator correlations also showed that a linear spring-damper representation of a tire-strut assumbly was adequate. The equivalent spring rates and damping coefficients for each airplane were also established based on these correlations and utilized in the present (LANRTO) simulation.

Reverse Thrust

Although no credit for engine reverse thrust is allowed in determining brake kinetic-energy absorption capacity for certification,[1-3] use of reverse thrust is an essential part of jet aircraft operation. During landing, thrust reversers are utilized on a routine basis to reduce brake wear and during adverse weather conditons to stop the airplane in available runway length. During the rare occurrence of a refused takeoff (RTO), thrust reversers are a must and sometimes provide the only retarding force. For these reasons, operators mandate that the thust-reverser capability (in terms of additional stopping capability) be included in the flight manual performance charts. Hence, it was considered essential to include the effects of reverse thrust in the analysis and it is provided as a user option in the program.

Conclusions

Previous brake-energy analysis required tedious hand calculations in a segmented form. The current analysis presents a computerized version of the Method II analysis of MIL-W-5013 and FAR 25 requirements. Additionally, its flexibility allows the user to account for nose-gear braking, flap setting, reverse thrust, and engine transients, among other things. The program can be utilized for brake sizing for

new airplanes and for evaluating and predicting stopping performance of existing airplanes.

Acknowledgment

This work was conducted under an IR&D Project funded by the Boeing Commerical Airplane Company. The author thanks the company for the permission to publish the paper.

References

[1] "Federal Aviation Regulations, Landing Gear, Wheels, Brakes and Tires," FAR Part 25, Sec. 25.721 through 25.735, May 1970.

[2] "Federal Aviation Regulations, Aircraft Wheels and Brakes," FAR Part 37, TSO-C26b, Jan. 1971.

[3] "Military Specification, Wheel and Brake Assemblies; Aircraft," MIL-W-5013H, April 1971.

[4] Creech, D. E., "Aircraft Brake-Energy Analysis Procedures," Aeronautical Systems Division, Wright-Patterson AFB, Ohio, ASD-TR-68-56, Oct. 1968.

[5] "SAE Aerospace Recommended Practices, Wheels, and Brakes," ARP-597A, July 1963.

[6] Wahi, M. K., Warren, S. M., Amberg, R. L., Straub, H. H., and Attri, N. S., "Combat Traction II, Phase II," Technical Rept. No. ASD-TR-74-41, Vol. 1, The Boeing Company, Oct. 1974.

[7] Wahi, M. K., "Application of Dimensional Analysis to Predict Airplane Stopping Distance," *Journal of Aircraft*, Vol. 14, Feb. 1977, pp. 209-214.